Environment Canada
Environnement Canada

Institut National de Recherche sur les Eaux

APPLICATION OF A SIMPLE NUMERICAL WAVE PREDICTION MODEL TO LAKE ERIE[4]

by

David J. Schwab[1], John R. Bennett[2], Paul C. Liu[2], and Mark A. Donelan[3]

Inland Waters Directorate
Direction Générale des Eaux Intérieures

This manuscript has been accepted by the

Journal of Geophysical Research, Oceans

APPLICATION OF A SIMPLE NUMERICAL WAVE PREDICTION MODEL TO LAKE ERIE[4]

by

David J. Schwab[1], John R. Bennett[2],
Paul C. Liu[2], and Mark A. Donelan[3]

[4]GLERL Contribution No. 382

[2]Great Lakes Environmental
Research Laborator/NOAA
230 Washtenaw Avenue
Ann Arbor, Michigan 48104

[3]Shore Processes Section
Hydraulics Division
National Water Research Institute
Canada Centre for Inland Waters
Burlington, Ontario
January 1984

Abstract

A parametric dynamical wave prediction model has been adapted and tested against semianalytic empirical results for steady conditions in a circular basin and extensive field measurements of wave height, period, and direction. The adapted numerical model accurately predicts the directional spreading of waves for uniform steady wind that Donelan (1980) had predicted analytically for fetch-limited waves. When the model was applied to the central basin of Lake Erie and the results compared to observations of wave height and period (at two points in the lake) and direction (at one point), results for wave height and direction estimates were excellent compared to measurements at a research tower off the southern shore, but computed wave heights were lower than observed at a weather buoy in the western part. The model somewhat underestimated wave periods at both places. Thus, with locally measured wind data as input, the model estimates wave height and direction well and wave period acceptably.

RÉSUMÉ

On a modifié un modèle paramétrique dynamique de prévision des vagues dont on a comparé les résultats aux résultats empiriques semi-analytiques obtenus pour des conditions stables dans un bassin circulaire ainsi qu'à d'importantes mesures en situation de la hauteur, de la periode et de la direction des vagues. Le modèle numérique modifié prédit avec précision la direction de propagation des vagues soulevées par un vent uniforme constant que Donelan (1980) avait prédit analytiquement pour des vagues limitées par le fetch. Lorsque le modèle a été appliqué au bassin central du lac Érié et que les résultats ont été comparés aux observations de la hauteur, de la période (en deux points du lac) et de la direction (en un point) des vagues, les résultats étaient excellents comparativement aux mesures effectuées à une tour de recherche au large de la rive sud, mais les hauteurs calculées des vagues étaient inférieures à celles observées à une bouée météorologique dans la partie ouest. Par conséquent le modèle prédit bien la hauteur et la direction, et d'une manière acceptable, la période des vagues à partir de mesures locales du vent comme données d'entrée.

MANAGEMENT PERSPECTIVE

This paper reports on the assessment of the Donelan wave prediction model, developed at NWRI, which gives height, period and direction, by scientists at the Great Lakes Environmental Research Laboratory, NOAA, in the United States.

The report concludes that the model predicts waves in lakes accurately provided the wind data is of acceptable quality.

Donelan's model marks a significant advance in wave prediction technique and it will be adopted in Lake Erie by the U.S. National Oceanic and Atmospheric Administration. This model should be used for all lakes where wave data is required provided the lake is deep. More work is necessary for shallow water lakes.

T.M. Dick
Chief
Hydraulics Division

PERSPECTIVE DE GESTION

Cette communication porte sur l'évaluation, par les scientifiques du Great Lakes Environmental Research Laboratory, NOAA, aux États-Unis, du modèle de prévision des vagues de Donelan qui donne la hauteur, la période et la direction des vagues.

Le rapport conclut que le modèle fournit des prévisions précises sur les vagues dans la mesure où les données sur le vent sont d'une qualité acceptable.

Le Modèle de Donelan constitue un progrès important en matière de prévision des vagues et sera adopté par la National Oceanic and Atmospheric Administration des États-Unis pour le lac Érié. Il devrait être utilisé pour tous les lacs sur les vagues desquels des données sont nécessaires pourvu que ces lacs soient profonds. D'autres travaux sont nécessaires dans le cas des lacs aux eaux peu profondes.

T.M. Dick

Chef de la Division de l'hydraulique

1. INTRODUCTION

Numerical wave prediction models can be categorized according to their developments as spectral or parametric or as a combination of both. The spectral models [e.g., Pierson, Tick, and Baer, 1966; Barnett, 1968; Resio, 1981] are based on the concept that the evolution of the wave spectrum is given by an energy transport equation. The energy is split into spectral components, with discrete frequencies traveling in certain direction bands. Source terms, consisting of energy input from the atmosphere, energy loss, and redistribution of energy due to nonlinear interactions, are taken from theoretical or empirical formulations. The parametric models [e.g., Hasselmann et al., 1976; Gunther et al., 1979] solve the same energy transport equation, but make assumptions about the spectral shape to reduce the problem to the prediction of a few nondimensional parameters. The drawback to this type of model is that, under rapidly changing wind conditions, the shape of the wave spectrum may vary significantly from the parametric representation. Gunther et al. [1981] made further developments to incorporate changing wind direction. Golding [1983] developed a system to combine a parametric technique for predicting wind waves with a discrete spectral model for swell.

In this paper, we present an encouraging test of a parametric model developed by Donelan [1977]. It differs from other parametric models in two ways. First, the basic equation is a local momentum balance equation rather than an energy transport equation. Momentum input results from drag on the waves which depends on wave height and the difference between wave speed and wind speed. Second, the model has provisions for a "fossil" wave field that may be left behind by a rapidly changing wind. This second feature is particularly important in the Great Lakes, where multipeaked wave spectra are sometimes observed.

The model was tested against Lake Erie data obtained in September and October 1981. Two sets of data are available. The first consists of nearly continuous measurements of wind speed and direction; air temperature; water temperature; and wave height, period, and direction at a tower 6 km off the southern shore of the Lake [Schwab, et al. 1984]. The second is from a satellite-reporting NOAA Data Buoy Center (NDBC) NOMAD buoy moored in the western part of the central basin and includes all of the above parameters except wave direction. The model results agree very well with wave height and direction measurements at the tower. A systematic deviation of wave direction from wind direction for certain wind directions is apparent in both the tower observations and the model results. Wave period agreement at the tower is satisfactory. Wave height measurements at the buoy are consistently higher than the model results, although the correlation is high. Reasons for the discrepancy in wave height at the NOMAD buoy are not presently clear. Wave period agreement at the buoy is again satisfactory. The conclusion is that, given accurate wind information, the model can provide excellent forecasts of wave height and direction and satisfactory forecasts of wave period at any point in the lake.

2. THE NUMERICAL MODEL

The Donelan (1977) numerical wave forecast model is based on conservation of momentum applied to deep water waves. On the assumption of equipartition of potential and kinetic energy in the wave field, the x and y momentum components are:

$$M_x = g \int_0^{\infty} \int_0^{2\pi} \frac{F(f,\theta)}{C(f)} \cos\theta \, d\theta \, df \qquad (1)$$

$$M_y = g \int_0^{\infty} \int_0^{2\pi} \frac{F(f,\theta)}{C(f)} \sin\theta \, d\theta \, df \qquad (2)$$

where $F(f,\theta)$ is the wave energy spectrum as a function of frequency, f, and direction, θ, and $C(f)$ is the phase speed. The rate of change of momentum is related to input from the wind and divergence of the wave momentum flux:

$$\frac{\partial M_x}{\partial t} + \frac{\partial T_{xx}}{\partial x} + \frac{\partial T_{xy}}{\partial y} = \frac{\tau_x^w}{\rho_w} \tag{3}$$

$$\frac{\partial M_y}{\partial t} + \frac{\partial T_{yx}}{\partial x} + \frac{\partial T_{yy}}{\partial y} = \frac{\tau_y^w}{\rho_w} \tag{4}$$

If we assume that the deep water linear theory applies, the group velocity is one-half the phase velocity and the components of the momentum flux tensor are:

$$T_{xx} = \frac{g}{2} \int_0^\infty \int_0^{2\pi} F(f,\theta)\cos^2\theta \, d\theta \, df \tag{5}$$

$$T_{xy} = T_{yx} = \frac{g}{2} \int_0^\infty \int_0^{2\pi} F(f,\theta)\sin\theta \cos\theta \, d\theta \, df \tag{6}$$

$$T_{yy} = \frac{g}{2} \int_0^\infty \int_0^{2\pi} F(f,\theta)\sin^2\theta \, d\theta \, df \tag{7}$$

If we further assume that the wave energy is distributed about the mean angle, θ_0, as cosine squared and there is no energy for $|\theta - \theta_0| > \pi/2$:

$$F(f,\theta) = \frac{2}{\pi} E(f) \cos^2(\theta - \theta_0) \tag{8}$$

and that θ_0 is independent of frequency, then the momentum fluxes can be expressed in terms of θ_0 and the variance:

$$\sigma^2 = \int_0^\infty E(f)df. \tag{9}$$

The integration of Equations (5)-(7) yields:

$$T_{xx} = g\left(\frac{\sigma^2}{4}\cos^2\theta_0 + \frac{\sigma^2}{8}\right) \tag{10}$$

$$T_{xy} = T_{yx} = g\left(\frac{\sigma^2}{4}\cos\theta_0 \sin\theta_0\right) \tag{11}$$

$$T_{yy} = g\left(\frac{\sigma^2}{4}\sin^2\theta_0 + \frac{\sigma^2}{8}\right) \tag{12}$$

These formulas are interesting for two reasons. First, they are independent of the shape of the spectrum. Second, $\sigma^2/8$ is an isotropic term. This term causes a wave pressure gradient from areas of high waves toward areas of low waves. To complete the formulation of the left-hand side of Equations (3)-(4) requires a relation between the variance, σ^2, and the momentum components. We assume the wave spectrum obeys the average JONSWAP formula [Hasselmann et al., 1973]:

$$E(f) = \alpha g^2(2\pi)^{-4}f^{-5}\exp\frac{-5}{4}\left(\frac{f}{f_p}\right)^{-4} \cdot 3.3^{\exp\left[-\frac{(f-f_p)^2}{2\beta^2 f_p^2}\right]} \tag{13}$$

$$\beta = \begin{cases} .07 : f < f_p \\ .09 : f > f_p \end{cases} \tag{14}$$

The two parameters are the peak frequency, f_p, and the Phillips equilibrium range parameter, α. From the JONSWAP empirical relations relating these to fetch, Donelan [1977] eliminated fetch to obtain a relation between the two:

$$\alpha = 0.0097 \left(\frac{U}{C_p}\right)^{2/3} \tag{15}$$

where $C_p = \frac{g}{2\pi f_p}$, and U is the 10-m wind speed.

Using this formula and integrating the JONSWAP formula yields (approximately):

$$\frac{\sigma^2}{|M|} = \frac{c_p}{g} \tag{16}$$

and

$$\sigma^2 = 0.30\alpha g^2 (2\pi)^{-4} f_p^{-4} \tag{17}$$

where $|M|$ is the magnitude of the momentum vector (M_x, M_y).

Turning now to the right-hand side of Equations (3)-(4), we require a formulation of the source of momentum to the waves. In this paper, we use the Donelan (1977) formulation:

$$\frac{\vec{\tau}_w}{\rho_w} = 0.028 D_f \left|\vec{U} - 0.83\vec{C}_p\right| (\vec{U} - 0.83\vec{C}_p) \tag{18}$$

In this formula D_f is the form drag coefficient defined here as $D_f = [0.4/\ln(50/\sigma)]^2$ with σ in meters. The factor of 0.028 is the empirical fraction of the stress that is retained by the waves.

As in all parametric models, several implicit assumptions have been made to obtain the simple form of the equations given here. So that the reader is fully aware of the assumptions and the attendant limitations of the model, we list them here.

(1) Equipartition of kinetic and potential wave energies.

(2) Propagation according to deep water linear theory.

(3) Cosine squared spreading.

(4) JONSWAP spectral shape.

(5) JONSWAP empirical dependence of α on non-dimensional fetch.

(6) JONSWAP empirical dependence of non-dimensional peak frequency on non-dimensional fetch.

(7) The input of wind momentum to waves follows the same law whether the waves are being driven by the wind, preceed the wind, or are adverse to it.

(8) When the wind and wave directions differ by more than $\pi/2$, the wind starts generating a new wave field in its direction. The old ("fossil") field propagates independently according to the same rules as the active field. As the wind (or waves) changes direction, the components of both fields are combined or the field interchanges names according to a set of rules that amount to defining "fossil" as the wave momentum, generated previously, which differs in propagation direction from that of the wind by more than $\pi/2$.

The limitations corresponding to the above assumptions are:

(1) While non-linearities in the wave field will reduce the validity of this assumption, this will make little difference to the predictability of the model, since the relationship between wind momentum and retained wave momentum is obtained experimentally from the wind stress and the variance of surface elevation. The latter is linearly proportional to the potential energy density and is the basic measure of wave energy in any measurement program. Thus, the inexactness of this assumption will be absorbed in the tuning of the parameter in (18) that corresponds to the fraction of wind momentum retained by waves.

(2) The assumption of the linear deep water dispersion relation is subject to two sources of error: (a) shallow water effects and (b) amplitude dispersion. The former introduces some error near the shores, but since the average depth of Lake Erie is 20 m and observed periods are generally 6.5 seconds or less, the errors are probably less than those introduced by the coarse spatial definition of the wind field. Amplitude dispersion can increase phase and group speeds by as much as 10%. However, such large increaes occur only at the extremely small non-dimensional fetches charactersitic of laboratory experiments. Increases of up to 3% are characteristic of young lake waves, but until a clear relationship between wave age and mean amplitude dispersion has been obtained experimentally, there seems little point in attempting a correction of this size.

(3) The directional spreading of wind waves is a subject of current controversy. While it is now clear that a cosine squared distribution is too wide, there is some disagreement about a more appropriate form or even whether pitch-roll buoys are capable of sufficient directional resolution to establish the correct form. In the interest of simplicity of exposition, we have used the traditional cosine squared distribution until the matter is more clearly resolved.

(4) The JONSWAP spectral shape was used since it was derived from fetch-limited data, which are characteristic of the Great Lakes. However, as the waves approach full development, the peak enhancement of the spectrum should become less pronounced until, at full development, the spectrum should be in agreement with the well-established Pierson-Moskowitz (1964) spectrum. The JONSWAP spectrum, with its constant peak enhancement, does not have this property. One effect of this would be that the period of

waves approaching full development will be underestimated since the enhanced peak allows the computed energy to be sufficiently large although the period is too small.

(5) The equilibrium range parameter α in the JONSWAP spectrum was estimated by fitting the rear face of the spectrum to a frequency power law with exponent -5. It now appears that an exponent of -4 or even a variable may be more appropriate. (See, for example, Kitaigorodskii, 1983; Liu, 1983.) Clearly a new equilibrium range parameter is needed and its dependence on non-dimensional fetch recomputed from the original spectra. Such an enterprise is beyond the scope of this paper, but it seems likely that such a fundamental redefinition of the spectral form will affect the predictability of the model.

(6) Phillips (1977) has pointed out that the JONSWAP empirical dependence of non-dimensional peak frequency on non-dimensional fetch includes laboratory data in which the "balance of dynamical processes appears to be rather different from those in the field." He argues that only field data should be used in establishing an empirical relation of this sort. While we agree, we used the original JONSWAP relations as a consistent set, leaving aside the testing of model sensitivity to choice of empirical functions until we have acquired a more comprehensive wind data set.

(7) Miles' (1957, 1959, and 1967) theory of wave amplification of wind is commonly invoked to provide the form of wind input to the waves. The amplitude is increased severalfold from that given by Miles' theory to tune the models to the data. Of course, according to this theory there is no coupling with the waves if the waves either outrun the wind or run adverse to it--a result at variance with common observation and

occasional measurements. (See, for example, Stewart and Teague, 1980.) Clearly, there is a need for careful observation and controlled experimentation to sort out this important aspect of wave prediction. In the meantime, we have taken the view that wave-induced pressure fluctuations in the air are largely due to form drag, and the vectorial expression (18) applies, whatever the angle between wind and waves. Support for this approach comes from the laboratory experiments of Banner and Melville [1976] and the numerical modeling of Al-Zanaidi and Hui [1983].

(8) The separation of the wave fields into "active" and "fossil" is an attempt to deal with the handling of swell in a purely parametric model. A more realistic approach is to use a hybrid model in which the discrete swell components are allowed to propagate independently. In the Great Lakes, where swell is transitory and is relatively unimportant energetically, the enormous increase in computing time demanded by a hybrid model does not seem warranted. Instead, we conserve momentum, while allowing the immediate generation of new waves following a large wind shift, by storing it in the fossil field, which can be eroded by the wind even as the active field grows. Without the fossil field, the wind would have to demolish the adverse waves before generating new waves, a requirement clearly at variance with observations.

The numerical integration scheme is very simple. Forward time differences are used to forecast the momentum components at the centers of the elementary grid squares from the discrete forms of Equations (3) and (4). The stress components are evaluated from Equations (10) and (12) at the edges of the grid squares using a combination of upwind and centered differences. Then Equations (15)-(17) are used to determine the variance, σ^2, and the peak frequency, f_p, from the momentum components and the wind.

3. PRELIMINARY MODEL TESTS

The numerical model described in the previous section was tested for consistency with Donelan's [1980] manual formulas for wave height and wave direction for purely fetch-limited waves. These formulas have been validated with data from selected cases during the 1972 IFYGL experiment by Bishop [1983]. The formulas can be expressed as [Bishop, 1983]

$$H_c = 0.00366\, g^{-0.62} X^{0.38} (U \cos\theta)^{1.24} \tag{19}$$

where θ is the angle between the wind and the wave determined by maximizing the effective fetch, F_e, defined as:

$$F_e = X(\cos\theta)^{2.35} \tag{20}$$

Here X is fetch (which depends on θ) and H_c is the characteristic wave height, defined as four times the standard deviation, σ, of the surface fluctuation. The idea that fetch-limited waves need not travel in the direction of the wind is relatively new, but follows directly from the observations that 1) the two-dimensional wave spectrum consists of waves traveling in various directions, 2) the most energetic waves in the spectrum generally have the longest periods, and 3) the longest period waves arrive from the direction for which F_e is a maximum. Donelan [1980] gives examples of the distribution of F_e with wind direction for elliptical basins.

The numerical model was run on a 5-km grid representation of a 100-km diameter circular lake with a steady 10 m/s wind for 24 h. The height and direction of the two-dimensional wave field are plotted in Figure 1 as

dark-headed arrows. An arrow the length of the side of a grid square would represent a significant wave height of 1.5 m. The maximum wave heights at the eastern end of the basin are 1.2 m. Another set of arrows with length and direction determined by Equations (19) and (20) is plotted in Figure 1 with open arrowheads. With the exception of a few points near the upwind shore, the numerical results are virtually indistinguishable from the empirical fetch-limited formulas. The directional differences at the upwind shore are a result of the imperfect representation of the circular geometry in the numerical model and are not considered important. Figure 2 shows the profile of characteristic wave height along the diameter of the basin aligned with the wind. The dashed line corresponds to Equation (19) and the solid line is the result from the numerical computation. Again, the agreement is excellent. The main result of the test is that for uniform wind conditions the directional spreading of the wave field and the predicted significant wave heights in the numerical model are consistent with the fetch-limited formulas [Eqs. (19)-(20)].

4. DATA

The wave model was tested against data from two locations in Lake Erie for September and October 1981. In the eastern part of the central basin, the Great Lakes Environmental Research Laboratory (GLERL) was operating a solar-powered research tower approximately 6 km off the southern shore in 14 m of water. (See Figure 3.) Three Zwarts wave gages were mounted on the tower in an equilateral triangular array 2 m on a side, with a fourth gage at the center of the triangle to measure wave direction. Wind speed and direction, along with air temperature, were measured at 10 m. Water temperature was

measured 2 m below the surface. Wave spectra were calculated for a 10-min record once every half hour and other parameters were averaged over this period. Only hourly values of the observations are used in this comparison however. Schwab et al. [1984] describe the experiment in detail and give a climatological overview of the data. The tower instrumentation system is fully described in Schwab et al. [1980].

In the western part of the central basin, wave height, wave period, wind speed at 5 m, wind direction, air temperature, and water temperature were reported by a NDBC NOMAD buoy. (See Figure 3.) The NOMAD buoy is boat-shaped, 6.22 m in length with a 2.95 m beam. Wave parameters were measured by an accelerometer mounted on a vertically stabilized frame in the buoy and reported hourly. A detailed discussion of the NDBC buoy system and its calibration can be found in Steele and Johnson [1977].

The spectra based on recorded data from GLERL tower and NDBC buoy were calculated with 32 and 24 degress of freedom respectively. According to Donelan and Pierson (1983) the significant wave height and peak energy frequency estimated from the calculated spectrum are within ±10-15% and 5% of their respective true values.

5. RESULTS

The 5-km grid shown in Figure 3 was used to run the numerical model described in Section 2 for September and October 1981. The wind field was allowed to vary linearly along the longitudinal axis of the lake, matching the observed 10-m wind exactly at the NDBC buoy and at the GLERL tower. The profile method and a computer subroutine developed by Bennett et al. [1983] were used to determine the 10-m wind from the 5-m observation at the buoy. Linear interpolation in time was used between hourly wind observations.

Hourly values of significant wave height computed by the model are compared to measured values at the tower and at the NDBC buoy in Figures 4 and 5 and Table 1. The agreement at the tower is excellent, with a root mean square error of 0.20 m and a correlation coefficient of 0.93 between computed and observed values. At the buoy, the correlation coefficient is high (0.88), but the linear regression slope of 0.68 differs rather significantly from the tower result of 0.99. It suggests that the observed values at the buoy might be too high. This could result from either overestimated wave height measurements or underestimated wind speed measurements input to the model. Since we have no reason to doubt the validity of the wind data, further experiments comparing the calibration of different wave gages would be useful.

Computed and observed values of wave period at the tower and at the NDBC buoy are compared in Figures 6 and 7 and Table 2. At the tower, wave period is determined from the frequency corresponding to the maximum peak in the energy spectrum. At the buoy, NDBC reports both "average" period and "dominant" period. We used the "dominant" period for model comparison. The model calculates period as

$$T = \frac{2\pi C_p}{g}$$

where C_p is the phase velocity of the "active" component of the wave field. From Table 2 we see that the computed wave period systematically underestimates the observed periods. The root mean square errors of 1.16 s at the tower and 0.94 s at the buoy are not unacceptable, but may indicate that the JONSWAP empirical relations used in the model could be modified for further improvement. The excess peak enhancement of the JONSWAP spectrum (see Section

2) as full development is approached certainly accounts in part for the increasingly underestimated period values as period increases.

Wave direction measurements were only available from the GLERL tower. Figure 8a shows the differences of up to 50° between observed wave direction and wind direction that systematically occur for certain wind directions. Figure 8b shows the computed differences. It is clear that the deviations of wave direction from wind direction in the model are very similar to the observed deviations. Figure 9 compares computed and observed wave direction at the tower directly. The largest differences are for waves traveling in an offshore direction (90°-180°). These are probably the smallest waves, corresponding to extremely short fetch (6-10 km). For reasons discussed in Section 3, the model results for wave direction are not expected to be very accurate for these cases. In addition, it is more difficult to determine the wave direction accurately from the tower data for small wavelengths. The overall agreement between the computed and observed directions outside this range is excellent however.

6. CONCLUSIONS

The Donelan (1977) numerical wave model provides excellent estimations of wave height and direction (which may be different from wind direction) at any point in a lake as long as accurate wind measurements are available. The formulation of momentum source terms in this model is conceptually and operationally simpler than in other parametric and spectral models. Although the theoretical basis for the mathematical formulation of the wind-wave problem is far from understood at present, the combination of physical and empirical realizations used in this model appears to be well-suited to application on the Great Lakes. The sensitivity of the model to the assumptions listed in

Section 2 is being further tested against a more comprehensive wind and wave data set from Lake Ontario. Encouraged by the results of the present study, we plan to develop the model to include shallow water effects as well.

REFERENCES

Al-Zanaidi, M. A., and W. H. Hui, Turbulent air flow over water waves--A numerical study, submitted to J. Fluid Mech., 1983.

Banner, M. L., and W. K. Melville, On the separation of air-flow over water waves, J. Fluid Mech., 77, 825-842, 1976.

Barnett, T. P., On the generation, dissipation and prediction of ocean waves, J. Geophys. Res., 73, 513-530, 1968.

Bishop, C. T., Comparison of manual wave prediction models, J. Waterway, Port, Coast. Ocean Eng., ASCE, 109, 1-17, 1983.

Bennett, J., A. H. Clites, and D. J. Schwab, A two-dimensional lake circulation modelling system: Programs to compute particle trajectories and the motion of dissolved substances, NOAA Tech. Memo. ERL-GLERL-46, 51 pp., National Technical Information Service, Springfield, Va. 22151, 1983.

Donelan, M. A., A simple numerical model for wave and wind stress prediction, National Water Research Institute, Burlington, Ontario, 1977.

Donelan, M. A., Similarity theory applied to the forecasting of wave heights, periods, and directions, in Proceedings of the Canadian Coastal Conference, pp. 47-61, National Research Council, Ottawa, Ontario, 1980.

Donelan, M. A., and W. J. Pierson, The sampling variability of estimates of spectra of wind generated gravity waves, J. Geophys. Res., 88, 4381-4392, 1983.

Golding, B., A wave prediction system for real-time sea state forecasting, Quart. J. Royal Met. Soc., 109, 393-416, 1983.

Gunther, H., W. Rosenthal, T. J. Weare, B. A. Worthington, K. Hasselmann, and J. A. Ewing, A hybrid parametrical wave prediction model, J. Geophys. Res., 84, 5727-5738, 1979.

Gunther, H., W. Rosenthal, and M. Dunckel, The response of surface gravity waves to changing wind direction, J. Phys. Oceanogr., 11, 718-728, 1981.

Hasselmann, K., T. P. Barnett, E. Bouws, H. Carlson, D. E. Cartwright, K. Enke, J. A. Ewing, H. Gienapp, D. E. Hasselmann, P. Kruseman, A. Merrburg, P. Muller, D. J. Olbers, K. Richter, W. Sell, and H. Walden, Measurements of wind-wave growth and swell decay during the Joint North Sea Wave Project (JONSWAP), Deut. Hydrogr. Z., A12, 95 pp., 1973.

Hasselmann, K., D. B. Ross, P. Muller, and W. Sell, A parametrical wave prediction model, J. Phys. Oceanogr., 6, 201-228, 1976.

Kitaigorodskii, S. A., On the theory of the equilibrium range in the spectrum of wind-generated gravity waves, J. Phys. Oceanogr., 13, 816-827, 1983.

Liu, P. C., A representation for the frequency spectrum of wind-generated waves, Ocean Eng., 10, 429-441, 1983.

Miles, J. W., On the generation of surface waves by shear flows, J. Fluid Mech., 3, 185-204, 1957.

Miles, J. W., On the generation of surface waves by shear flows, Part 2, J. Fluid Mech., 6, 568-582, 1959.

Miles, J. W., On the generation of surface waves, Part 5, J. Fluid. Mech., 30, 163-175, 1967.

Phillips, O. M., The Dynamics of the Upper Ocean, 2nd edition. Cambridge University Press, 336 pp., 1977.

Pierson, W. J., and L. Moskowitz, A proposed spectral form for fully developed wind seas based on the similarity theory of S. A. Kiraigorodskii, J. Geophys. Res., 69, 5185-5190, 1964.

Pierson, W. J., L. J. Tick, and L. Baer, Computer based procedures for preparing global wave forecasts and wind field analysis capable of using wave data obtained from a spacecraft, paper presented at the Sixth Symposium on Naval Hydrodynamics, Office of Naval Research, Washington, D.C., 1966.

Resio, D. T., The estimation of wind-wave generation in a discrete spectral model, J. Phys. Oceanogr., 11, 510-525, 1981.

Schwab, D. J., P. C. Liu, H. K. Soo, R. D. Kistler, H. L. Booker, and J. D. Boyd, Wind and wave measurements taken from a tower in Lake Michigan, J. Great Lakes Res., 6, 76-82, 1980.

Schwab, D. J., G. A. Meadows, J. R. Bennett, H. Schultz, P. C. Liu, J. E. Campbell, and H. H. Dannelongue, The response of the coastal boundary layer to wind and waves: Analyis of an experiment in Lake Erie, submitted to J. Geophys. Res., 1984.

Steele, K., and A. Johnson, Jr., Data buoy wave measurements, in Ocean Wave Climate, edited by M. D. Earle, pp. 301-316, Plenum Press, New York, N.Y., 1977.

Stewart, R. H., and C. Teague, Dekameter radar observations of ocean wave growth and decay, J. Phys. Oceanogr., 10, 128-143, 1980.

FIGURE LEGENDS

Fig. 1. Wave height and direction from numerical model (dark arrowheads) and empirical formulas (open arrowheads). Wind speed is 10 m/s, diameter of the basin is 100 km, duration is 24 h. An arrow length the same as the side of a grid square represents 1.5-m significant wave height.

Fig. 2. Characteristic wave height along the diameter of a circular basin aligned with a steady 10 m s^{-1} wind. The solid curve is the result from the numerical model, the dashed curve represents the empirical formula for wave height (Equation 19).

Fig. 3. Location of research tower and NOMAD buoy [NOAA Data Buoy Center (NDBC) buoy 45005] in Lake Erie. A 5-km computational grid is superimposed on the lake outline.

Fig. 4. Comparison of hourly computed and observed wave heights at GLERL tower for September and October 1981.

Fig. 5. Comparison of hourly computed and observed wave heights at NDBC buoy 45005 for September and October 1981.

Fig. 6. Comparison of hourly computed and observed wave period at GLERL tower for September and October 1981.

Fig. 7. Comparison of hourly computed and observed wave period at NDBC buoy 45005 for September and October 1981.

Fig. 8. Comparison of hourly wave and wind directions at GLERL tower for September and October 1981. a) observed, b) computed.

Fig. 9. Direct comparison of hourly computed and observed wave directions at GLERL tower for September and October 1981.

TABLE 1. Comparison of Computed and Observed Values of Significant Wave Height

	GLERL Tower	NDBC 45005
Number of points	890	1423
Observed:		
Mean	0.75 m	0.84 m
Standard deviation	0.52 m	0.47 m
Computed:		
Mean	0.74 m	0.61 m
Standard deviation	0.55 m	0.36 m
Correlation coefficient between computed and observed values	0.93	0.88
Root mean square error	0.20 m	0.33 m
Linear regression of computed values on observed values:		
Slope	0.99	0.68
Intercept	-0.002 m	0.03 m
Standard error	0.20 m	0.17 m

TABLE 2. Comparison of Computed and Observed Values of Wave Period

	GLERL Tower	NDBC 45005
Number of points	889	1427
Observed:		
Mean	4.16 s	3.65 s
Standard deviation	1.32 s	0.99 s
Computed:		
Mean	3.30 s	3.05 s
Standard deviation	1.26 s	0.95 s
Correlation coefficient between computed and observed values	0.81	0.72
Root mean square error	1.16 s	0.94 s
Linear regression of computed values on observed values:		
Slope	0.77	0.69
Intercept	0.09 s	0.52 s
Standard error	0.74 s	0.66 s

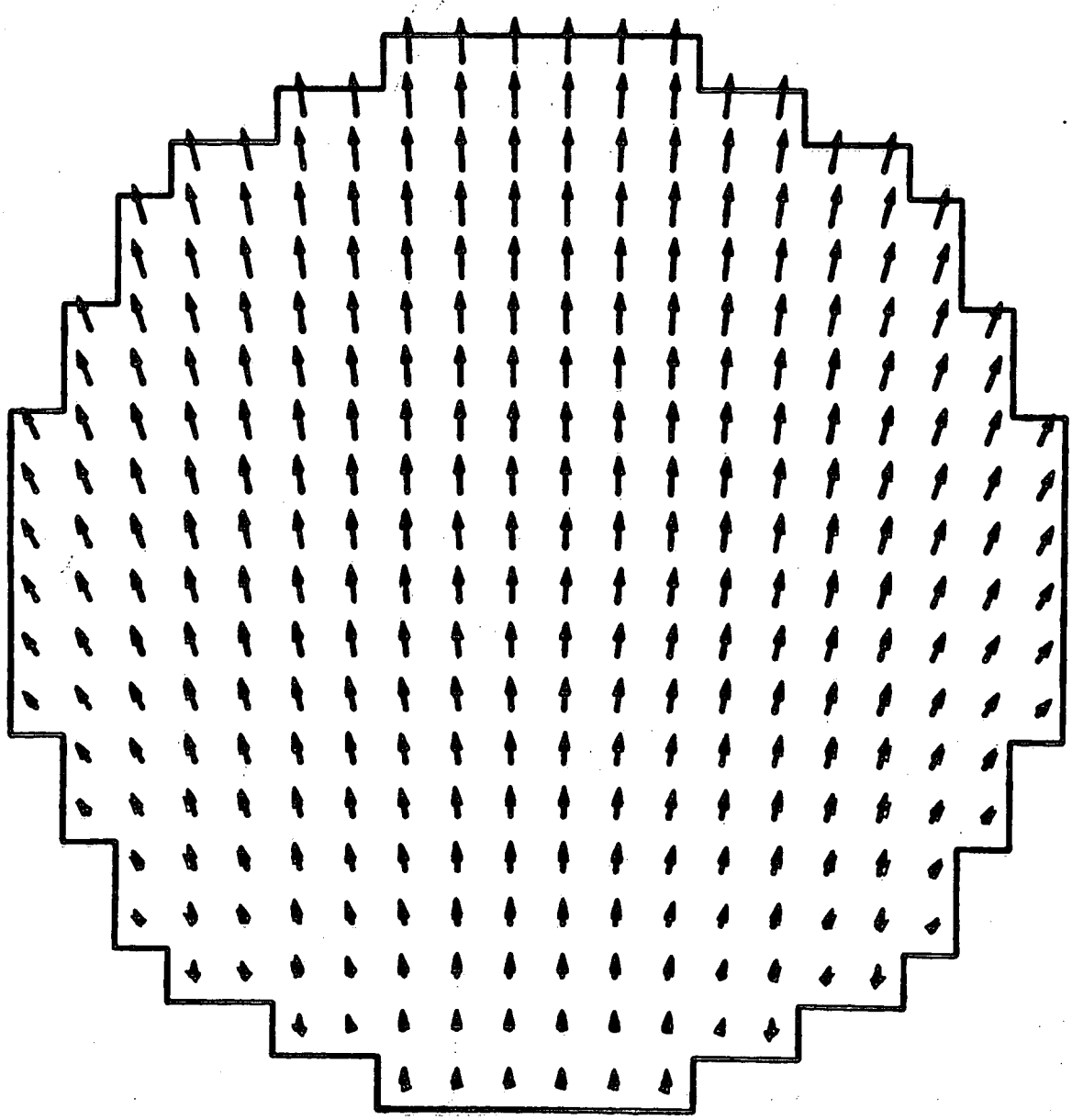

Figure 1

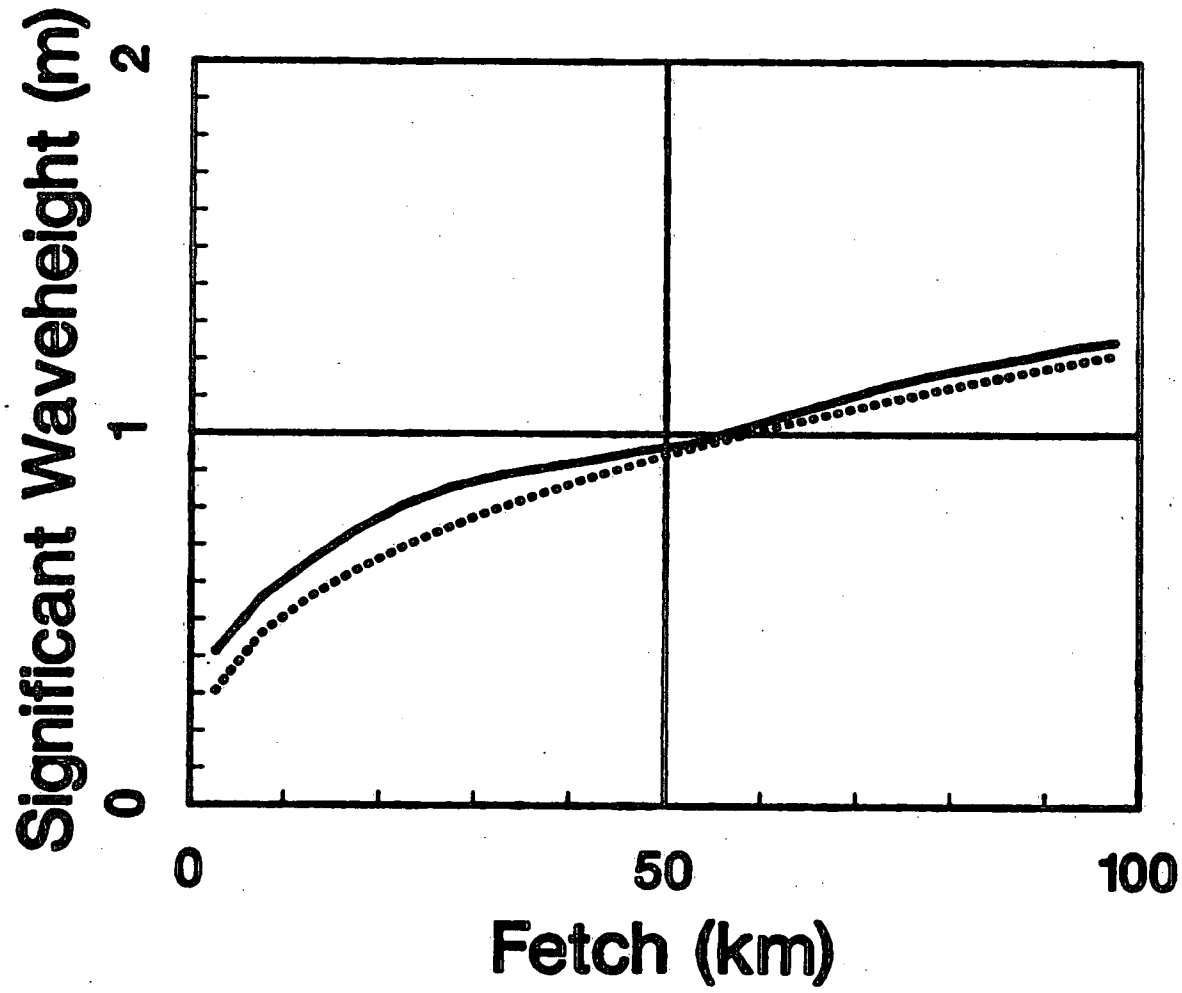

Figure 2

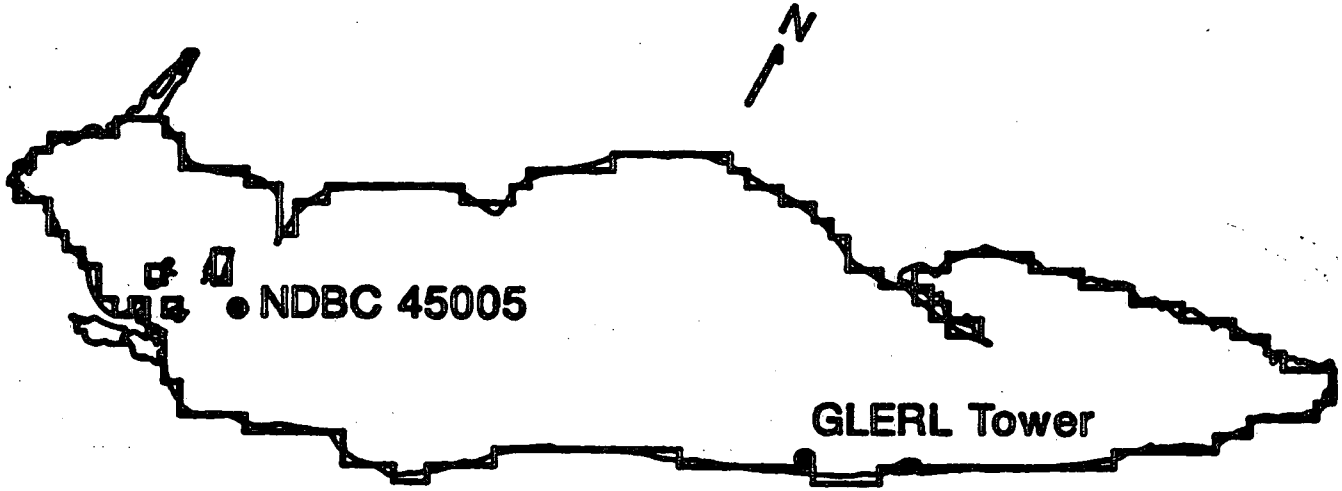

Figure 3

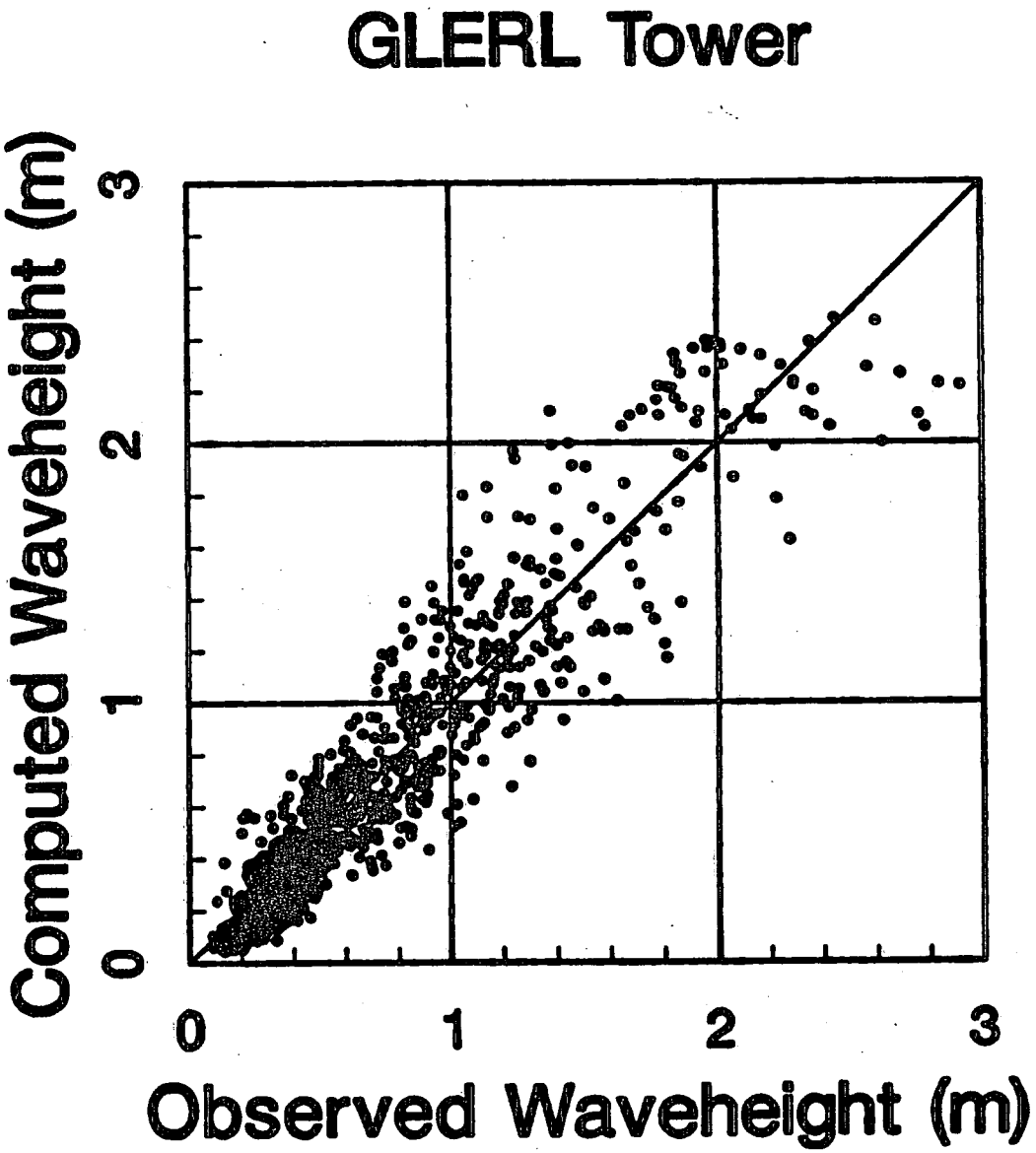
GLERL Tower
Computed Waveheight (m)
0
1
2
3
0
1
2
3
Observed Waveheight (m)

Figure 4

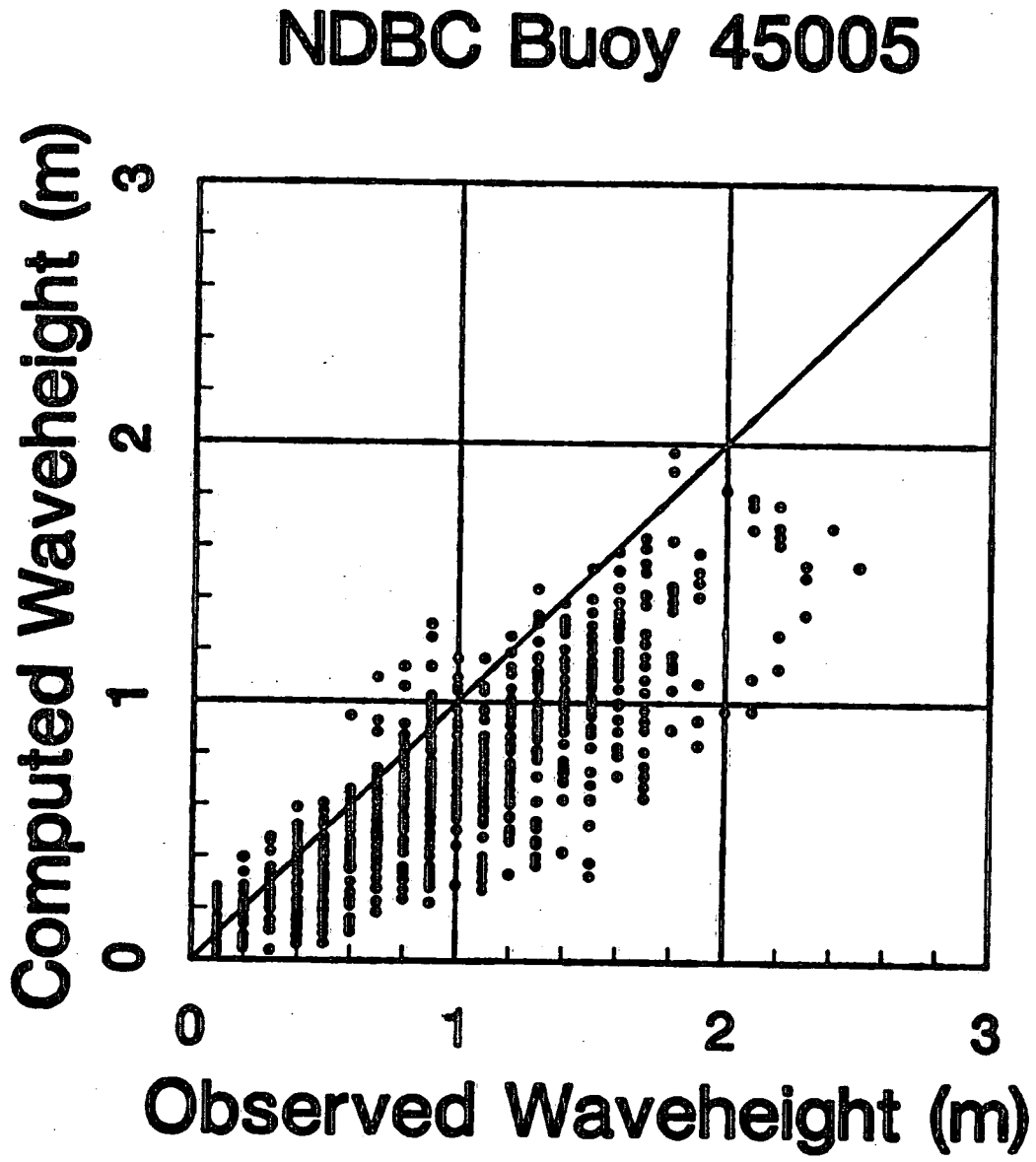
NDBC Buoy 45005
Computed Waveheight (m)
0
1
2
3
0
1
2
3
Observed Waveheight (m)

Figure 5

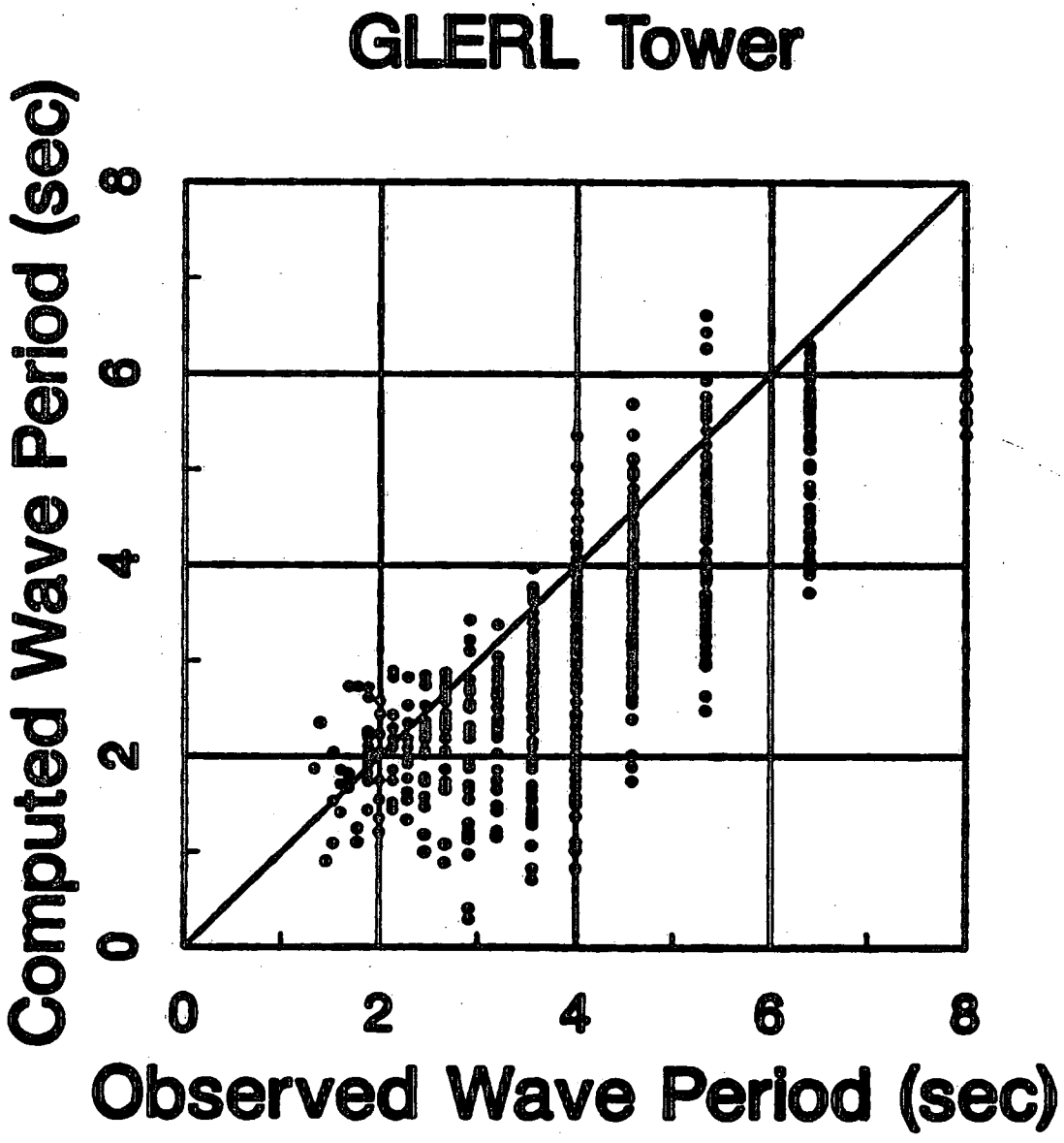
GLERL Tower
Computed Wave Period (sec)
0
2
4
6
8
Observed Wave Period (sec)

Figure 6

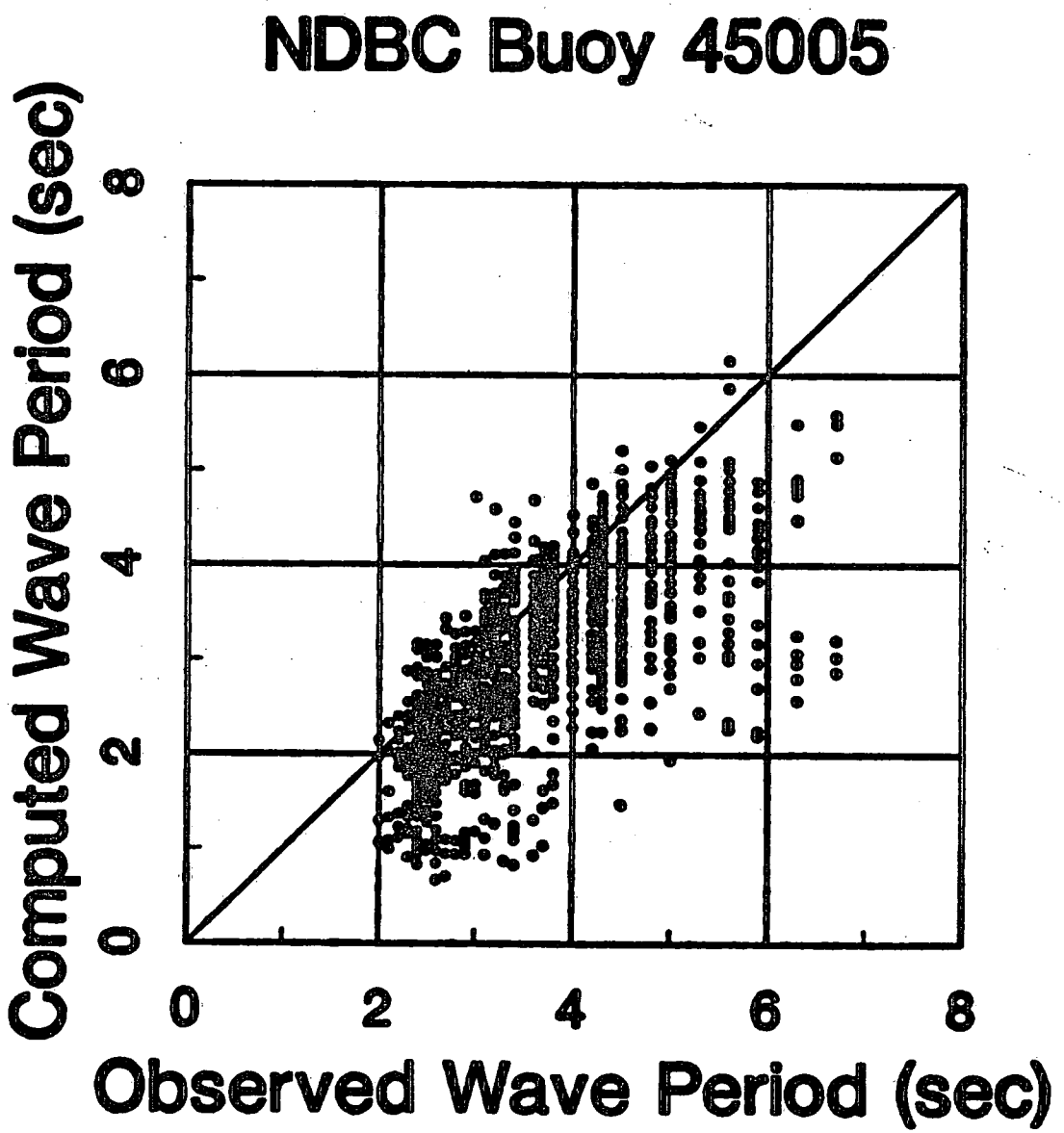
NDBC Buoy 45005
Computed Wave Period (sec)
0
2
4
6
8
0
2
4
6
8
Observed Wave Period (sec)

Figure 7

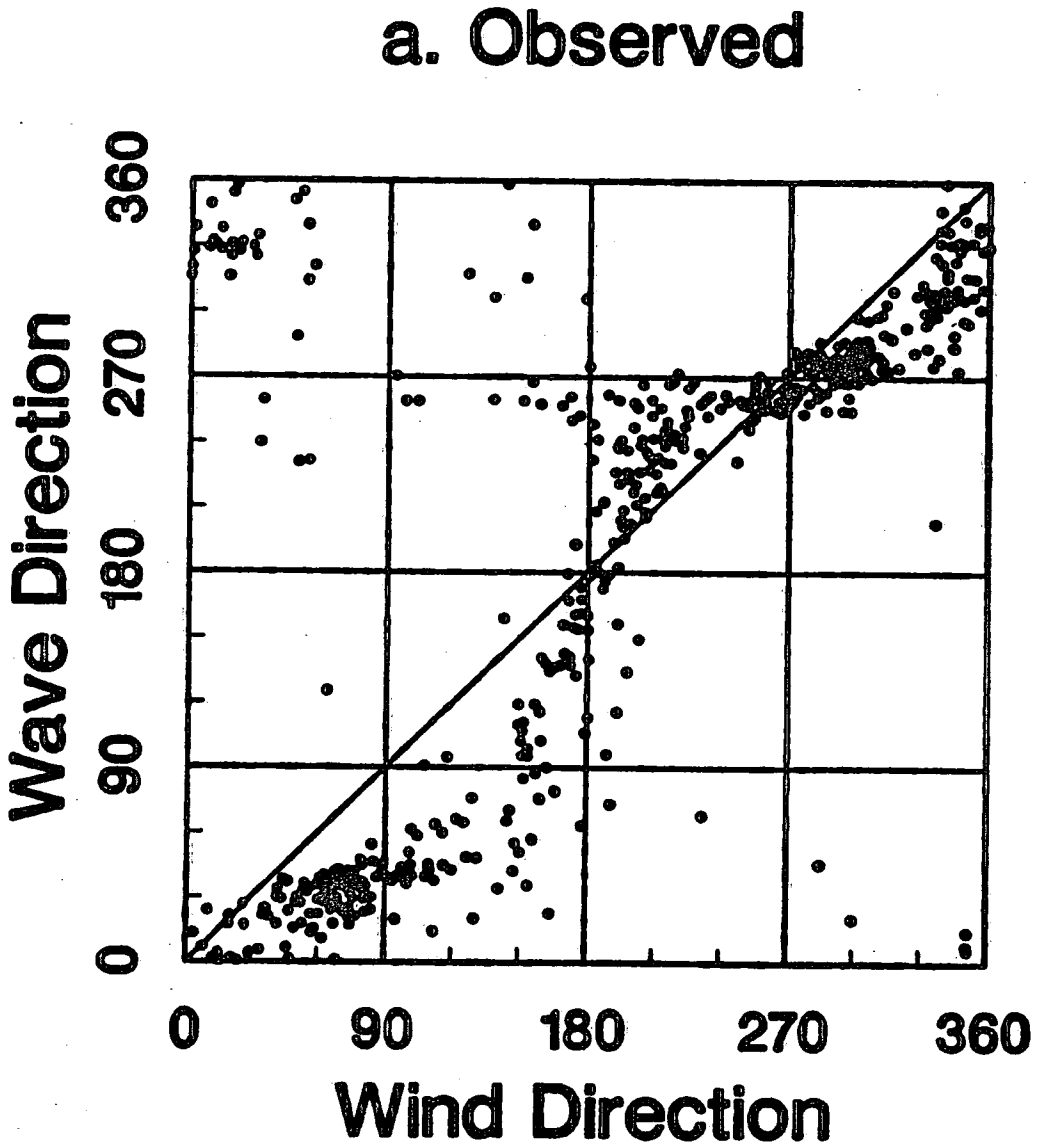
a. Observed
Wave Direction
0
90
180
270
360
0
90
180
270
360
Wind Direction

Figure 8

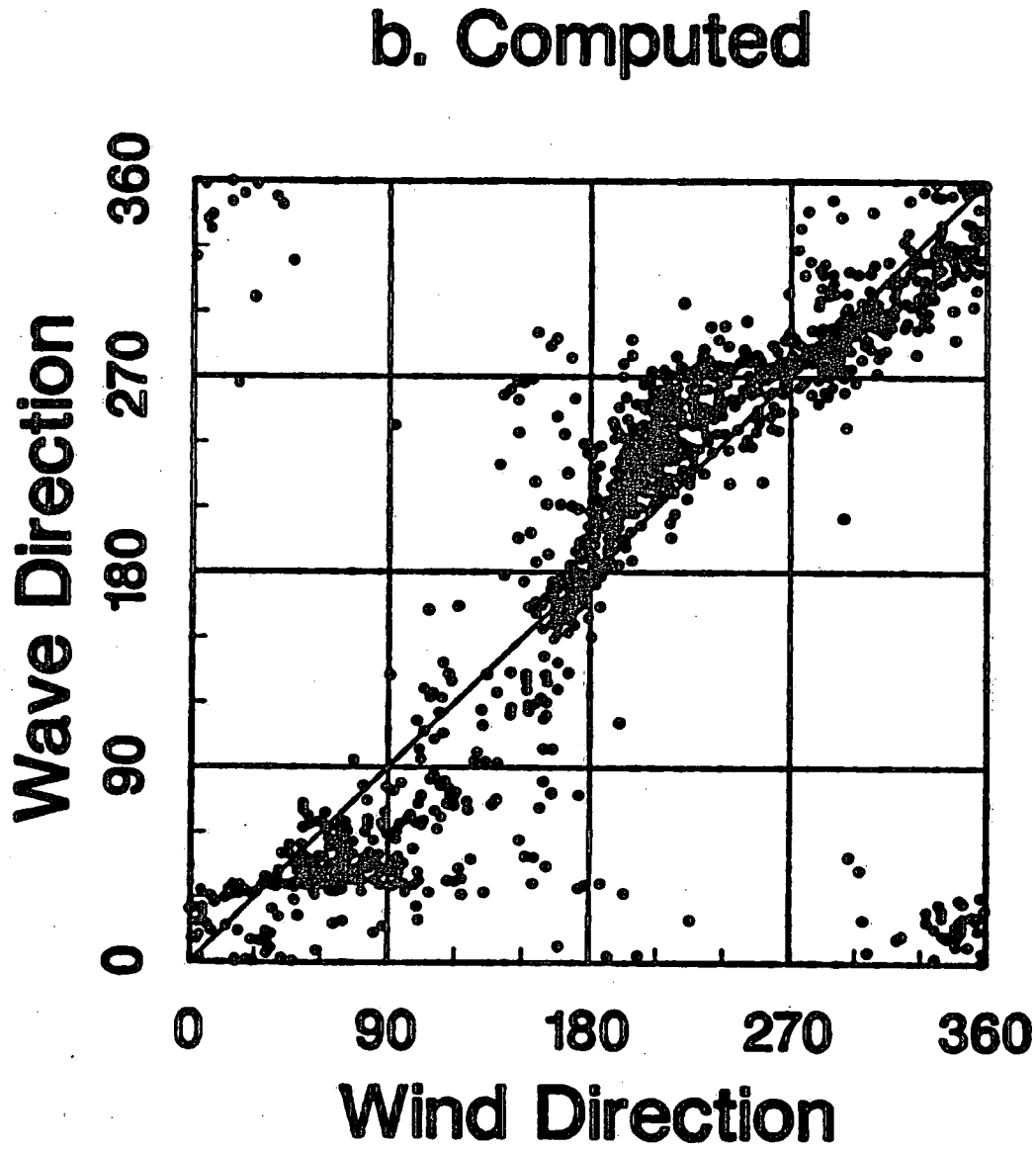
b. Computed
Wave Direction
0
90
180
270
360
0
90
180
270
360
Wind Direction

Figure 8

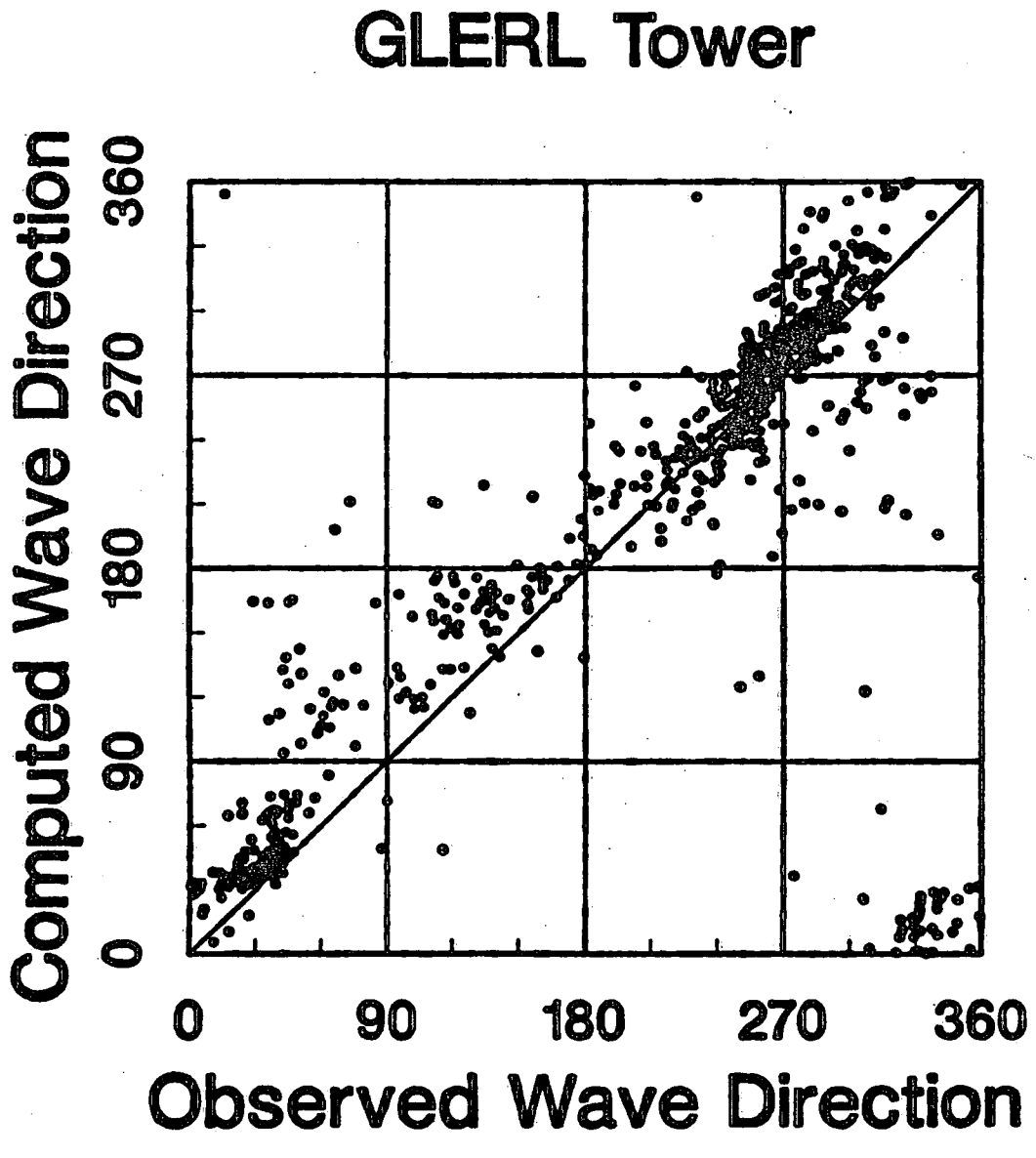
GLERL Tower
Computed Wave Direction
0
90
180
270
360
0
90
180
270
360
Observed Wave Direction

Figure 9

9947